Electronic supplementary information

Molecular interactions and functionalities of organic additive in a perovskite semiconducting device: a case study towards high performance solar cells

Hongkang Gong[a], Qi Song[a], Chao Ji[a], Huimin Zhang[a], Chunjun Liang[a*], Fulin Sun[a], Chenhui Zhang[a], Anqi Yang[b], Dan Li[b*], Xiping Jing[c], Fangtian You[a] and Zhiqun He[a*]

[a] *Key Laboratory of Luminescence and Optical Information, Ministry of Education, Institute of Optoelectronic Technology, Beijing Jiaotong University, Beijing, 100044, China*

[b] *Department of Physics, School of Science, Beijing Jiaotong University, Beijing, 100044, China*

[c] *College of Chemistry and Molecular Engineering, Peking University, Beijing 100871, P. R. China*

List of contents

* Corresponding authors: Z. He (zhqhe@bjtu.edu.cn), C. Liang (chjliang@bjtu.edu.cn), D. Li (danli@bjtu.edu.cn)

1. Experimental details:

Materials

PbI_2 (99.99%), $PbBr_2$(99.99%), $HC(NH_2)_2I$ (FAI, 99.5%) CH_3NH_3I (MAI, 99.5%), CsI (99.5%), were purchased from TCI; (S)-3-Amino-4-phenylbutyric acid hydrochloride (s-APACl, 98%) from Aladdin; Poly(triaryl amine) (PTAA) from Xi'an Polymer Light Technology; [6,6]-phenyl-C61-butyric acid methyl ester (PCBM) and Fullerene (C60) from Nano-C; 2,2'-(Perfluorocyclohexa-2,5-diene-1,4-diylidene)dimalononitrile (F4TCNQ) from TCI; zirconium acetylacetonate ($Zr(acac)_4$) from Sigma-Aldrich. All solvents, anhydrous dimethyl sulfoxide (DMSO, extra dry), *N*, *N*-dimethylformamide (DMF, extra dry), toluene, chlorobenzene and isopropanol (IPA) were purchased from Acros.

Perovskite precursor: a solution (1.4 M) was prepared by dissolving PbI_2 (567.9 mg), $PbBr_2$ (61.7 mg), FAI (210.4 mg), MAI (16.9 mg) and CsI (18.2 mg) in 1 ml mixed solvent (DMF/DMSO = 4/1) for a feed-in composition of $Cs_{0.05}(FA_{0.92}MA_{0.08})_{0.95}Pb(I_{0.92}Br_{0.08})_3$. It was further stirring at 60 °C for 12 hrs.

Perovskite precursor with s-APACl addtive: Dissolve s-APACl (1, or 3, or 5 mg) into 1 ml perovskite precursor for different fraction of additive. The s-APACl additive was added into the perovskite precursor 1 hr before films fabrication.

Device fabrication

ITO/glass were sequentially cleaned with soap, deionized water, ethanol under ultrasonication. The substrates were treated with UV ozone for 20 min. Perovskite films and devices were fabricated in a N_2 glove box. Hole-transport PTAA was dissolved in toluene at 10 mg ml^{-1} (with 1%(w/w) F4TCNQ) previously, which was spin-coated on ITO/glass substrates at 6000 r.p.m for 40 s and annealed at 150 °C for 10 min. A two-step spin-coating procedure with 1000 rpm for 10 s and 5500 r.p.m for 30 s was used to fabricate the perovskite films. Chlorobenzene (200 μl) was dropped on the spinning substrate at the last 10 s. The film was then annealed at 100 °C for 30 min. Electron-transport PCBM:C60 (1:1, w/w) was dissolved in dichloride benzene and spin-coated on perovskite/PTAA/ITO/glass substrate at 1000 rpm for 50s. $Zr(acac)_4$ dissolved in isopropanol was spin-coated on top of the electron transport layer at 4000 rpm for 40 s. Finally, Cu (80 nm) was deposited on top of $Zr(acac)_4$ as an electrode using thermally evaporating at 1.0×10^{-6} pa. The active areas of the devices were 0.04 cm^2.

Characterizations of materials

X-ray diffraction (XRD) patterns were taken using a diffractometer (Bruker D8 advance). Electron microscopic images and energy-dispersive X-ray spectroscopy (EDS) were obtained on a Scanning electron microscopy (SEM) (Hitachi S4800) working at a 15 kV and a distant of ~8 mm with 20k multiplication using a secondary electron mode. The surface morphologies of the films were measured via atomic force microscope (AFM) (Nanocute, SII NanoTechnology). Steady state photoluminescence (PL) spectra were measured using a fluorescence spectrometer (Horiba Nanolog FL3-2iHR). Time-resolved photoluminescence (TRPL) spectra were obtained with ultrafast lifetime spectrofluorometer (Horiba Delta flex). UV-Vis absorption spectra were taken with UV-Vis-NIR scanning spectrometer (Shimadzu UV-3101PC). Ultraviolet photoemission spectroscopy (UPS) measurement was measured with an angle-resolved photoemission spectrometer (VG Scienta R4000 energy analyzer) using a monochromatic He I light source ($h\upsilon$ = 21.22 eV) under a sample bias of -5V.

X-ray photoelectron spectroscopy (XPS) was tested via X-ray photoelectron spectrometer (Thermo escalab 250Xi). Infrared spectra were obtained via Fourier transform infrared spectrometer (FT-IR) (Nicolet IS 10). ^{1}H nuclear magnetic resonance spectra (^{1}H NMR) were measured on a NMR spectrometer (Bruker AVANCE III 600M). Decomposition temperature was tested using via a thermogravimetric analyzer (TGA) (TA instruments, Q600). Impedance of the materials was evaluated using an AC impedance analyzer (Solartron 1260) in frequency range from 1MHz to 0.1Hz at a voltage bias of 0.94V in the dark.

Device testing

Current-voltage (*J-V*) measurements of the devices were tested using a source meter (Keithley 2635B) under illumination of solar simulator (Abet Sun 2000) at a standard irradiation of AM 1.5G (100 mW/cm^2). These were measured at scanning rate of 10 mVs^{-1}. The external quantum efficiencies (EQE) of the solar cells were detected with a solar cell quantum-efficiency measurement system (Zolix Solar Cell Scan 100).

Conditions for operational stability tests are as follows:
In stability test, *J–V* characteristics were recorded automatically at one hour interval using a source meter (Keithley 2635B) under illumination of white LED unit at a standard irradiation of AM 1.5G (100 mW/cm^2) in a nitrogen filled glove box at room temperature. In operational stability test, a constant biased voltage (0.94 V) at the maximum power point (MPP) was also applied.

In this work, an "aged device" stands for the device after operational stability tests, i.e., after continuous illumination for 250 hours at 100 mW/cm^2 at room temperature with a bias voltage stress at the maximum power point (MPP) and *J-V* scan at one hour interval, which is in contrast to a "fresh device" (freshly prepared device).

An "Aged film" is the active perovskite layer prepared from the "aged device" by peeled-off the top "PCBM:C60/Zr(acac)$_4$/Cu" layers. This can be done by immersing the device into chlorobenzene for 10 minutes. The PCBM:C60 layers were dissolved and removed. The perovskite surface was then washed again by chlorobenzene to clean up any residual.

2. Thermal stability of s-APACl

s–APACl is a chiral organic in a powder form at room temperature having a melting temperature around ~ 150 ºC. Decomposition temperature of s-APACl was measured using thermogravimetric analysis (TGA), which is about 240 °C indicating that s-APACl is a thermally stable compound withstanding annealing process of perovskite at 100 °C.

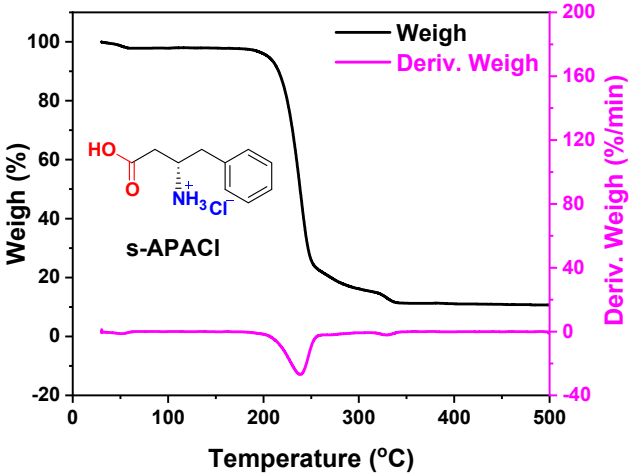

Figure S1 Thermogravimetric analysis spectra of s-APACl

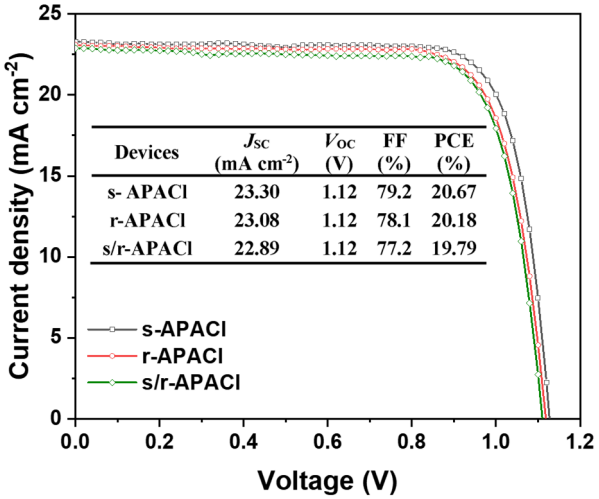

Devices	J_{SC} (mA cm^{-2})	V_{OC} (V)	FF (%)	PCE (%)
s- APACl	23.30	1.12	79.2	20.67
r-APACl	23.08	1.12	78.1	20.18
s/r-APACl	22.89	1.12	77.2	19.79

Figure S2. *J–V* characteristics of perovskite device have APACl additive of different chirality.

3. Devices testing using APACl additive of different chirality

Preliminary *J–V* measurement of perovskite devices fabricated using APACl of different chirality, s-APACl, r-APACl and a mixture of s-APACl and r-APACl at a ratio of 1:1 as seen in **Figure S2**. Device using homechiral s-APACl or r-APACl demonstrated a better performance.

4. SEM images of the active layers

Surface morphology of the control, APACl-1, APACl-3, and APACl-5 films observed using SEM shown in **Figure S3**.

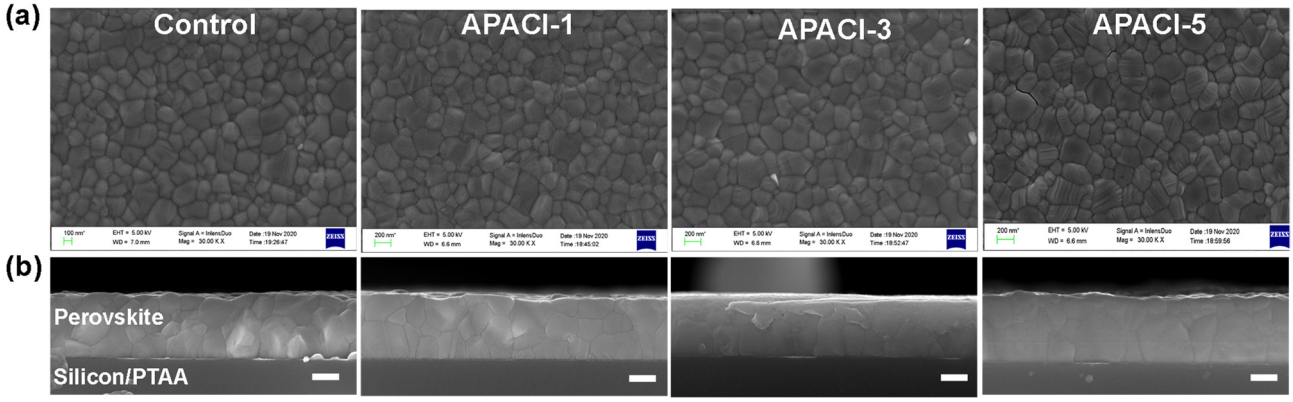

Figure S3 (a)Top view SEM pictures and (b) SEM images from cross-section view of control and 1, 3, 5 mg ml^{-1} s–APACl doped films.

5. AFM images and surface roughness of the active layers

AFM images of the control, APACl-1, APACl-3, and APACl-5 films are shown in **Figure S4**. The root-mean-square roughness (R_{RMS}) is 23.7, 22.5, 20.4 and 25.8 nm measured from the control, APACl-1, APACl-3, and APACl-5 films, respectively.

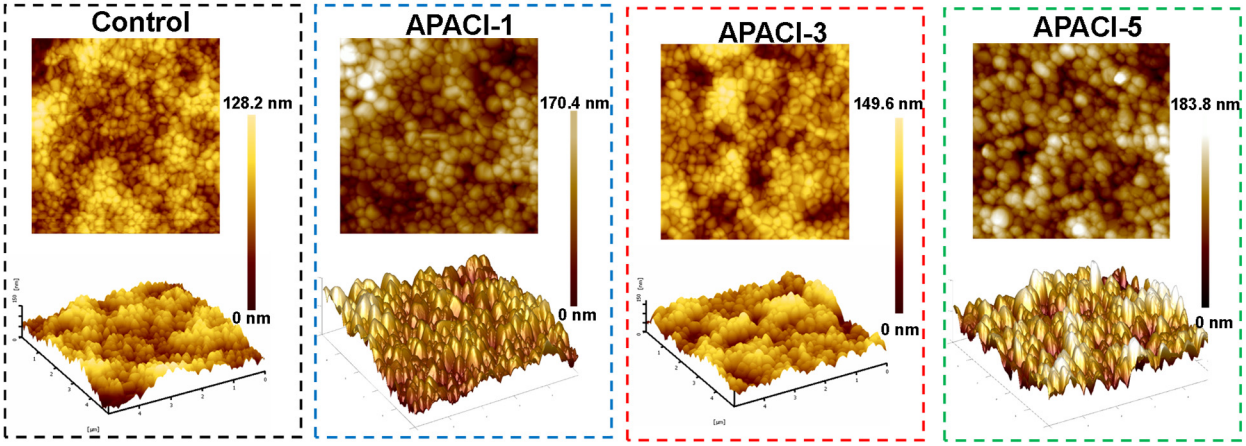

Figure S4 AFM morphology of the active films (Area 5 μm × 5μm)

6. UPS measurements of the active layers

UPS spectra were measured from the control, APACl-1, APACl-3, and APACl-5 layers as shown in Figure S5. Full data for energy band levels calculated are listed in **Table S1**.

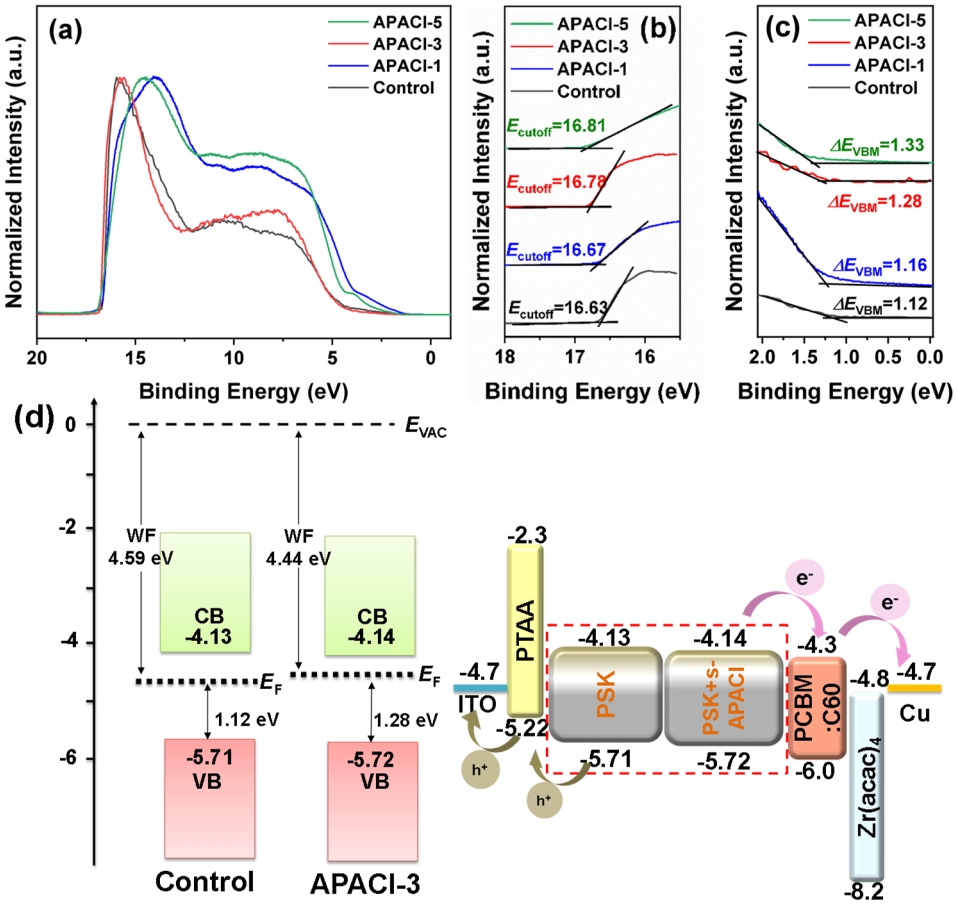

Figure S5 Full UPS plots (a), the secondary electron cutoffs (E_{cutoff}) (b), the valence band maxima (ΔE_{VBM}) (c), and a schematic energy diagram (d) of the control, APACl-1, APACl-3, and APACl-5 films

Table S1 Electronic energy levels of perovskite films obtained from UPS

Devices	E_{SEC} (eV)	E_g (eV)	W_F (eV)	ΔE_{VB} (eV)	E_{VB} (eV)	E_{CB} (eV)
Control	16.63	1.58	–4.59	1.12	–5.71	–4.13
APACl-1	16.67	1.58	–4.55	1.16	–5.71	–4.13
APACl-3	16.78	1.58	–4.44	1.28	–5.72	–4.14
APACl-5	16.81	1.58	–4.41	1.33	–5.74	–4.16

7. Time–resolved photoluminescence measurements

Table S2 Time–resolved photoluminescence

Devices	τ_1 (μs)	A_1 (%)	τ_2 (μs)	A_2 (%)	τ_{avg} (μs)
Control	0.37	45.2	0.69	54.8	0.59
APACl-1	0.66	54.4	1.59	45.6	1.28
APACl-3	1.19	72.8	2.86	27.2	1.98
APACl-5	1.88	80.0	5.01	20.0	3.11

A_i is the fraction of τ_i component. τ_{avg} is calculated from the equation $\tau_{avg} = \frac{\sum A_i \tau_i^2}{\sum A_i \tau_i}$

8. Steady-state power output of the devices

Steady-state power output of the control, APACl-1, APACl-3, and APACl-5 devices are shown in Figure S6.

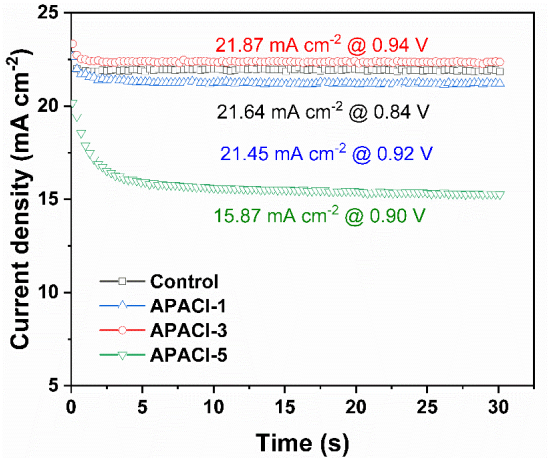

Figure S6. Steady-state power output at corresponding *J*sc measured at the maximum power point of the devices

9. Charts of photovoltaic parameters from of the devices

About 20 cells were measured for each condition to ensure the repeatability.

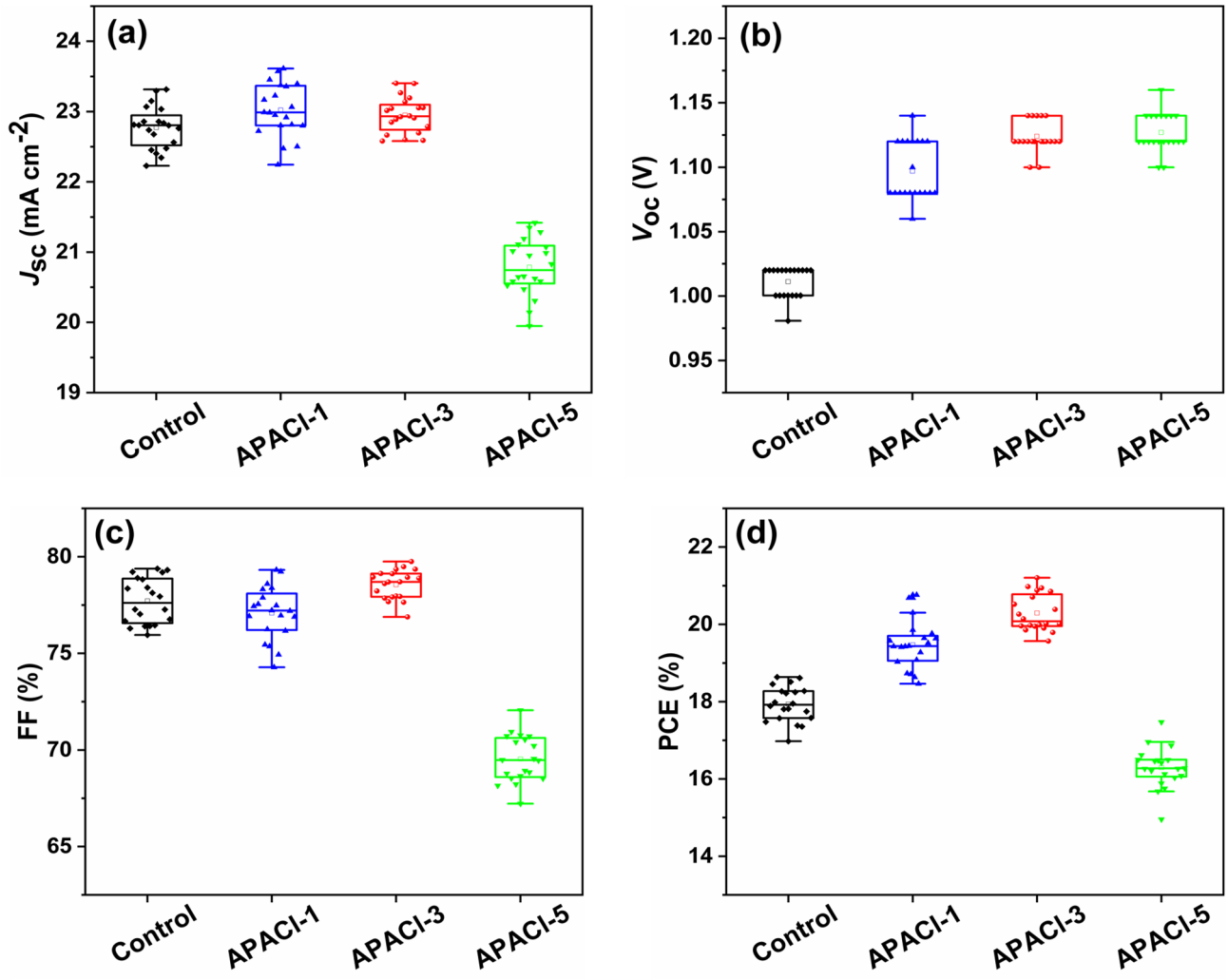

Figure S7 (a) J_{sc}, (b) V_{oc}, (c) FF and (d) PCE distribute diagram of the devices with 20 cells each. The center dot denotes mean value, box limits are upper and lower quartiles.

10. External quantum efficiency and dark *J-V* from the devices

External quantum efficiencies (EQE) of the control, APACl-1, APACl-3, and APACl-5 devices are shown in Figure S8(a). The integrating current densities obtained were 22.02, 22.1, 22.42, and 18.3 mA cm^{-2} from those devices, respectively, which were at a similar level to the short circuit current measured. Ideality factors (n) of the devices were also calculated from the dark J–V characteristics and change slightly against the voltage. Nevertheless, the n value from the control device appears to be ~ 2 or over, but that from APACl-3 device is the lowest around ~ 1.5.

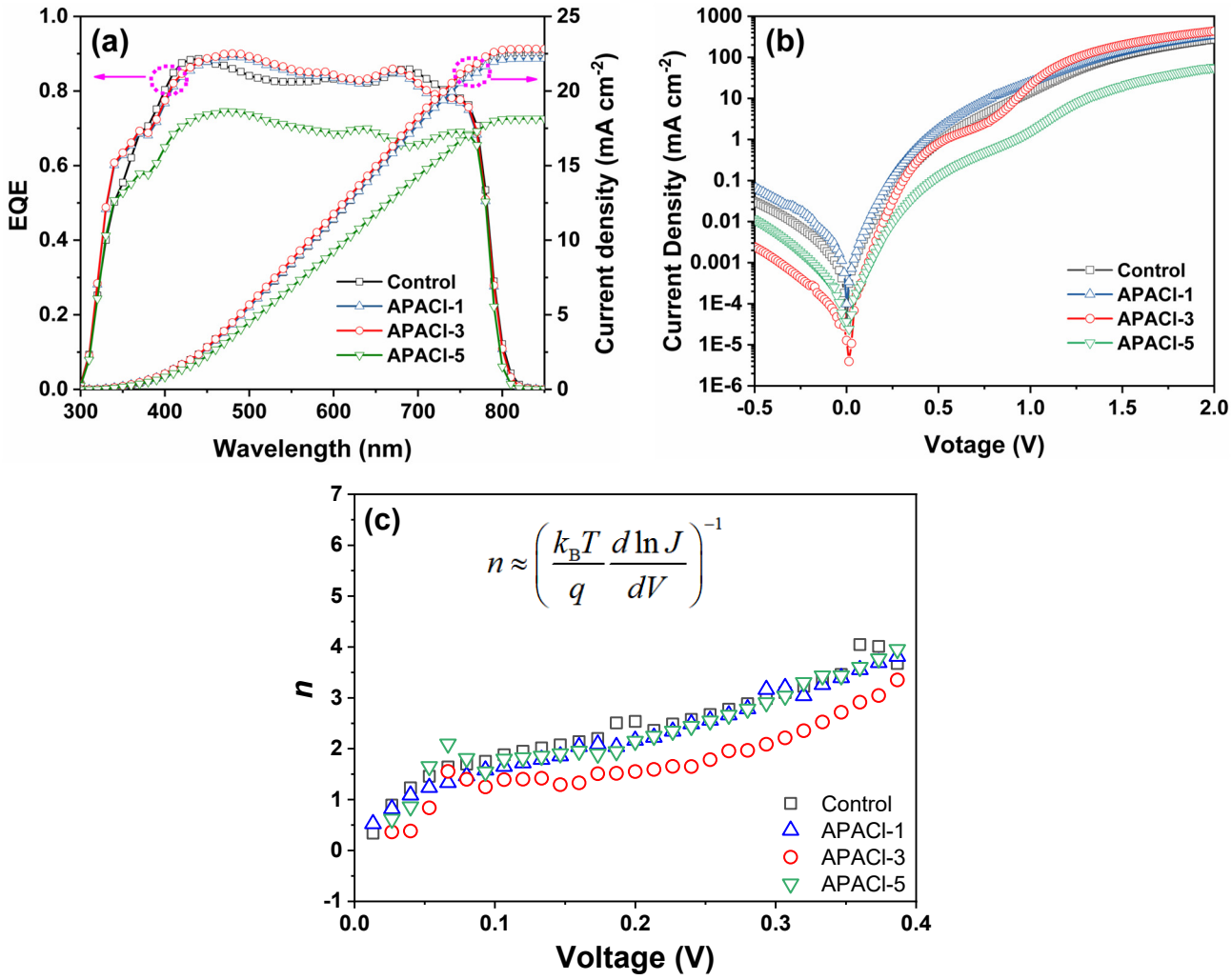

Figure S8. EQE spectra (a), dark J–V characteristics (b) and ideality factor n calculated from the dark J–V of the devices

11. FTIR spectra of PbI_2, s–APACl and the mixture

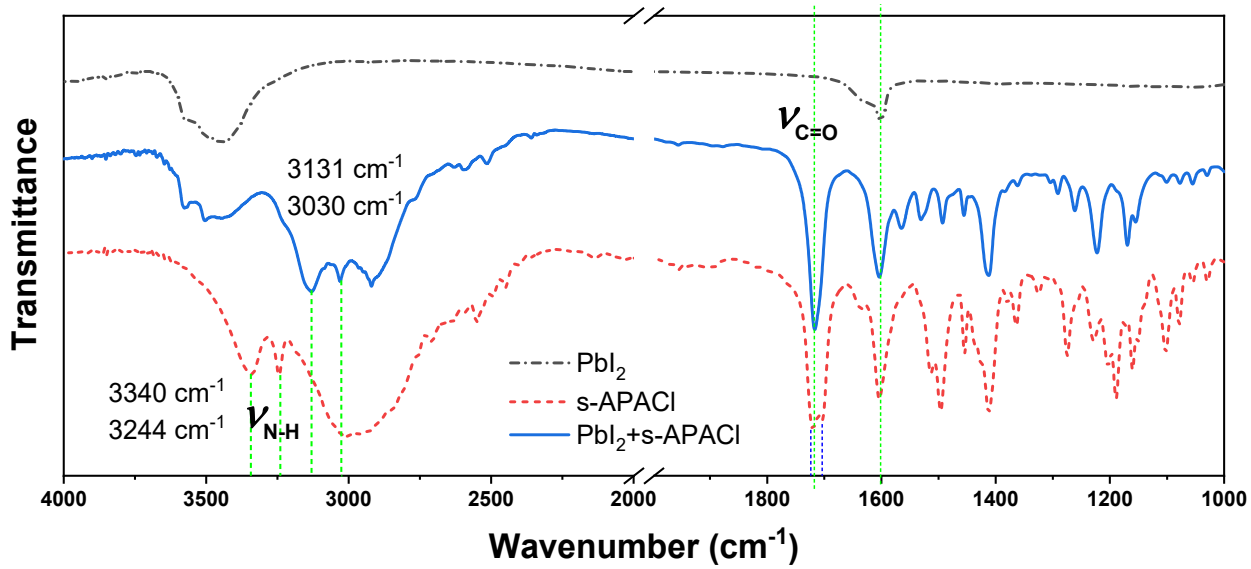

Figure S9. FTIR spectra of PbI_2, s–APACl and PbI_2+s–APACl powder

12. Photovoltaic parameters of the devices

Table S3 Photovoltaic parameters of reverse scan and forward scan for control and APACl-3 devices

Devices		J_{sc} (mA cm^{-2})	V_{oc} (V)	FF (%)	PCE (%)	H-index (%)
Control	Reverse	23.26	1.01	79.2	18.66	4.76
	Forward	22.91	1.01	76.7	17.77	
APACl-3	Reverse	23.30	1.12	78.2	20.41	3.57
	Forward	23.25	1.12	76.1	19.68	

H-index = (PCE_{RS} - PCE_{FS})/PCE_{RS}. RS: reverse scan, from 1.2 to 0 V; FS: forward scan, from 0 to 1.2 V

13. ^{1}H NMR spectra of s–APACl and the mixture with PbI_2

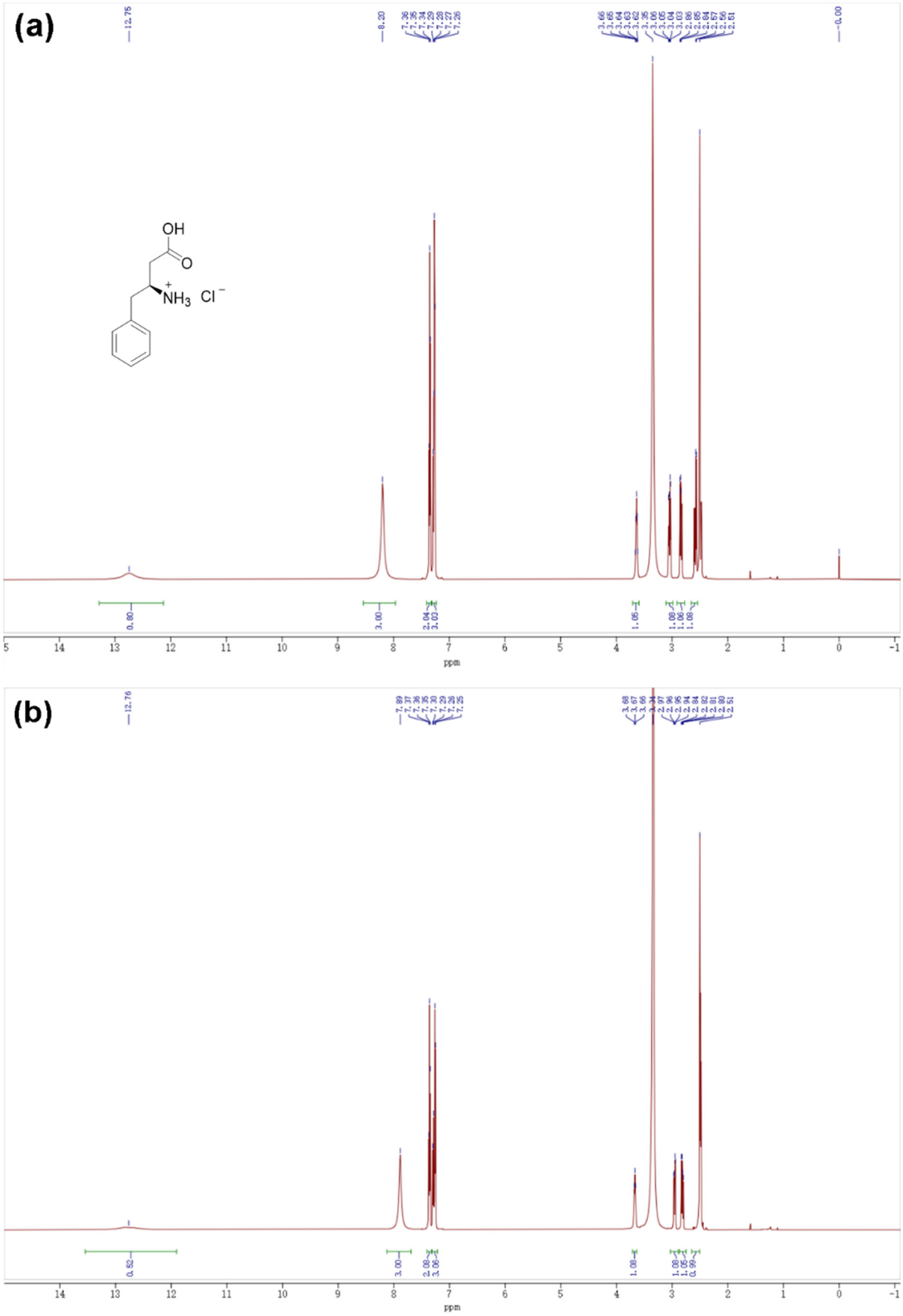

Figure S10 ^{1}H NMR spectra of (a) s–APACl and (b) s–APACl + PbI_2 (d_6-DMSO)

14. XPS spectra of control and s–APACl doped perovskite layers

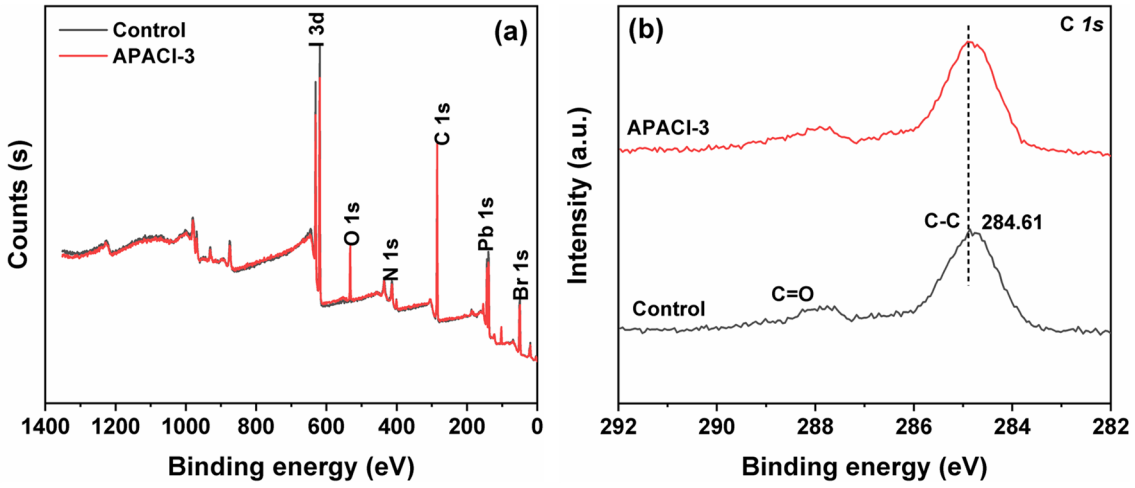

Figure S11 (a) XPS spectra of control and APACl-3 films; (b) C *1s* XPS spectra

15. SEM and EDS of fresh or aged perovskite devices

SEM images were taken from the crossed sections of "aged device" in comparison with "fresh devices" of either control or APACl-3.

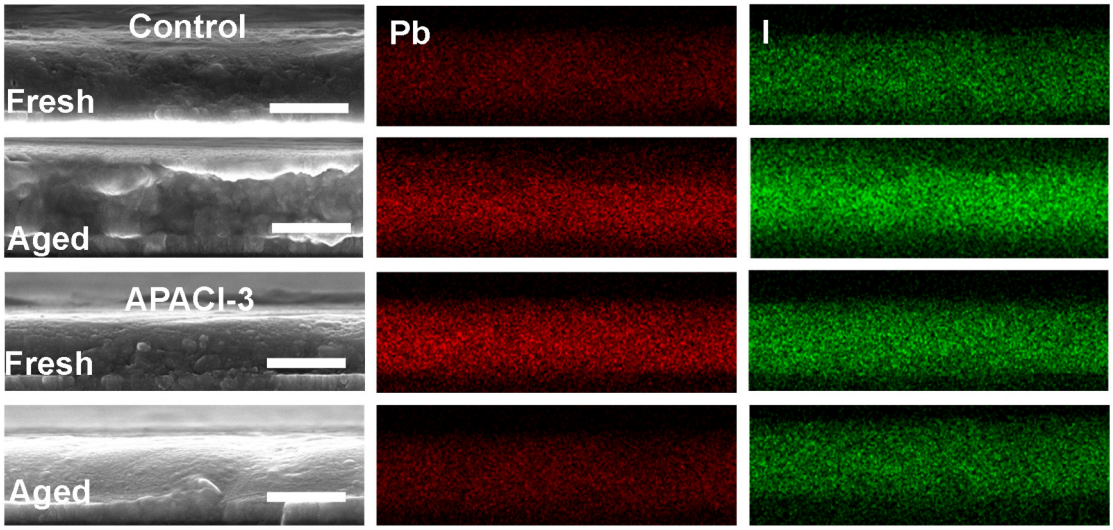

Figure S12 SEM images and EDS mapping cross section picture of fresh and 250h aged APACl-3 devices. The scale bars are 500 nm.